High-field phase diagram of the heavy-fermion metal $YbRh_2Si_2$

New Journal of Physics
The open-access journal for physics

High-field phase diagram of the heavy-fermion metal $YbRh_2Si_2$

P Gegenwart[1,3], Y Tokiwa[1], T Westerkamp[1], F Weickert[1], J Custers[1], J Ferstl[1], C Krellner[1], C Geibel[1], P Kerschl[2], K-H Müller[2] and F Steglich[1]

[1] Max Planck Institute for Chemical Physics of Solids, D-01187 Dresden, Germany
[2] Leibniz Institute for Solid State and Materials Research, IFW Dresden, D-01069 Dresden, Germany
E-mail: gegenwart@cpfs.mpg.de

New Journal of Physics **8** (2006) 171
Received 31 March 2006
Published 1 September 2006
Online at http://www.njp.org/
doi:10.1088/1367-2630/8/9/171

Abstract. The tetragonal heavy-fermion (HF) metal $YbRh_2Si_2$ (Kondo temperature $T_K \approx 25$ K) exhibits a magnetic field-induced quantum critical point related to the suppression of very weak antiferromagnetic (AF) ordering ($T_N = 70$ mK) at a critical field of $B_c = 0.06$ T ($B \perp c$). To understand the influence of magnetic fields on quantum criticality and the Kondo effect, we study the evolution of various thermodynamic and magnetic properties upon tuning the system by magnetic field. At $B > B_c$, the AF component of the quantum critical fluctuations becomes suppressed, and FM fluctuations dominate. Their polarization with magnetic field gives rise to a large increase of the magnetization. At $B^* = 10$ T, the Zeeman energy becomes comparable to $k_B T_K$, and a steplike decrease of the quasi-particle mass deduced from the specific-heat coefficient indicates the suppression of HF behaviour. The magnetization $M(B)$ shows a pronounced decrease in slope at B^* without any signature of metamagnetism. The field dependence of the linear magnetostriction coefficient suggests an increase of the Yb-valency with field, reaching 3+ at high fields. A negative hydrostatic pressure dependence of B^* is found, similar to that of the Kondo temperature. We also compare the magnetization behaviour in pulsed fields up to 50 T with that of the isoelectronic HF system $YbIr_2Si_2$, which, due to a larger unit-cell volume, has an enhanced T_K of about 40 K.

[3] Author to whom any correspondence should be addressed.

PII: S1367-2630(06)21724-5

Contents

1. Introduction

In lanthanide- and actinide-based heavy-fermion (HF) systems, the interplay between local on-site Kondo fluctuations and magnetic intersite interactions determines the ground-state behaviour [1]. Either long-range magnetically ordered or paramagnetic ground states occur, depending on the strength of the f-conduction electron hybridization. The latter can be varied by suitable changes in composition or by the application of pressure. However, the balance of the local and intersite interactions can also be modified by the application of magnetic fields. When the Zeeman energy becomes comparable to the thermal energy $k_B T_K$ of the Kondo fluctuations, the f-moment screening breaks down and local moment behaviour reappears. Correspondingly, long-range ordering is suppressed when the Zeeman energy exceeds the energy of the intersite-coupling strength. Furthermore, the application of a magnetic field will add a ferromagnetic (FM) component to the fluctuations. The influence of the applied field on the different components of the fluctuations will also depend on the single-ion anisotropy of the f-moments, e.g. Ising, planar or Heisenberg type. In Ising systems like $CeRu_2Si_2$ with pronounced magnetic anisotropy, the suppression of antiferromagnetic (AF) correlations by magnetic fields applied along the easy direction results in a pronounced metamagnetic transition accompanied by a substantial magnetostriction due to a strong magnetoelastic coupling [2].

In this paper, we study how magnetic fields affect the low-temperature properties of the tetragonal HF system $YbRh_2Si_2$ which has an easy-plane magnetic anisotropy [3]. This system is located very close at an AF quantum critical point (QCP). At zero magnetic field, it shows very weak AF ordering at $T_N = 70$ mK, which can be driven to zero by a small critical field $B_c = 0.06$ T applied perpendicular to the c-axis [4]. For $B > B_c$, Landau–Fermi liquid (LFL) behaviour is deduced from the electrical resistivity, described by $\rho(T) = \rho_0 + AT^2$. The coefficient $A(B)$ diverges for $B \to B_c$, indicating the presence of quantum critical fluctuations associated with the field-induced QCP [4]. Detailed studies have also been performed on $YbRh_2(Si_{1-x}Ge_x)_2$ with a nominal Ge concentration of $x = 0.05$ [5]. As pressure increases T_N for Yb-based systems, a slight volume expansion, induced by the partial substitution of Si-with the isoelectronic but larger Ge-atoms, suppresses T_N to 20 mK in $YbRh_2(Si_{0.95}Ge_{0.05})_2$. Correspondingly, the latter system has a tiny critical field of 0.027 T ($B \perp c$). When approaching the QCP either as a function of temperature at $B = B_c$, or from the LFL regime by reducing the field at low temperatures from $B > B_c$, thermodynamic and transport properties display strong non-Fermi liquid effects that are incompatible with the predictions of the standard Hertz–Millis theory for AF QCPs in itinerant systems [5, 6]. Motivated by these experiments, a new and

advanced model has been proposed which assumes the heavy quasi-particles to fractionalize at the QCP into (i) light electrons, (ii) bosonic spinons and (iii) spinless fermionic excitations [7]. To study the evolution of the Fermi surface volume upon tuning the system through the QCP, a detailed study of the low-temperature Hall resistance under differing field orientations has been performed [8]. Most interestingly, a large (40%) change of the Hall coefficient has been observed at B_c, although the ordered moment is tiny ($\sim 10^{-3}\mu_B$, only). This is in strong contradiction to a smooth evolution expected within the itinerant theory [9]. By contrast, the drastic change of the Hall coefficient upon tuning the system by field suggests at zero-temperature a sudden change of the Fermi surface at the QCP [8]. This would be compatible with a *locally critical* QCP where the heavy quasi-particles decompose due to the destruction of Kondo screening [9, 10].

The magnetic fluctuations of the system have been studied close to the QCP by bulk susceptibility [11], ^{29}Si nuclear magnetic resonance (NMR) [12], as well as Yb electron spin resonance (ESR) experiments [13]. Typically, the spin-fluctuation rates of Kondo ions cause large ESR linewidths making ESR signals undetectable. In $YbRh_2Si_2$, the first observation of ESR of the Kondo ion itself in a Kondo lattice system has been made. Most interestingly, the ESR signal occurs well *below* T_K and its intensity follows the temperature dependence of the bulk susceptibility which strongly increases upon cooling from high temperatures [13]. Several indications have been found that the quantum critical fluctuations have a strong FM component which dominates for $B > B_c$ [11]: (i) the Sommerfeld–Wilson ratio is highly enhanced with a value of about 20; (ii) except for temperatures below 0.3 K, the zero-field bulk susceptibility $\chi(T)$ shows divergent behaviour; (iii) the Pauli susceptibility $\chi_0(B)$ in the LFL regime diverges upon reducing the field towards B_c; (iv) the ratio A/χ_0^2 is field independent, unexpected for dominating AF fluctuations; and (v) the NMR-derived Korringa ratio is constant and has a value similar to that found in nearly FM metals [12]. Here, we focus on the high-field behaviour of $YbRh_2Si_2$. The evolution of bulk magnetic properties at small fields upon tuning the system through the QCP is documented in [11, 14].

The paper is organized as follows. Section 2 contains a description of the experimental methods. In section 3, we present zero-field specific-heat data and discuss the signatures of the Kondo effect and the weak AF ordering at low temperatures. Section 4 deals with experiments at $B > 0$ and discusses how the application of magnetic fields modifies the ground-state properties. The results are summarized in section 5.

2. Experimental

High-quality single crystals ($\rho_0 = 1\ \mu\Omega\,\mathrm{cm}$) were grown from In flux as described earlier [3]. Dilution refrigerators and superconducting magnets have been used for providing low temperatures and high magnetic fields, respectively. Standard techniques have been applied for electrical resistivity, specific-heat and magnetic ac-susceptibility experiments. For specific-heat measurements at temperatures above 1.5 K and fields up to 18 T, a commercial microcalorimeter from Oxford Instruments has been used. The magnetostriction has been detected by utilizing a high-resolution capacitive dilatometer. For the dc-magnetization measurements, a high-resolution capacitive Faraday magnetometer has been used [15]. Measurements under hydrostatic pressure were made with the aid of a miniaturized CuBe piston-cylinder pressure cell. The high-field magnetization has been studied at the pulsed-field facility at the Leibniz Institute for Solid State and Materials Research in Dresden up to 50 T [16]. To increase the mass of the investigated

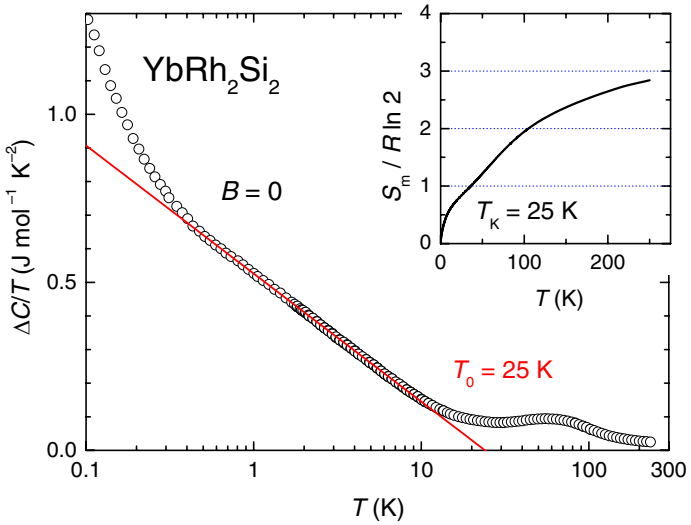

Figure 1. $4f$ increment to the specific heat of $YbRh_2Si_2$ as $\Delta C/T$ versus T (on a logarithmic scale) [3]. The red solid line indicates $\log(T_0/T)$ dependence with $T_0 = 25$ K. The inset displays magnetic entropy obtained from integrated $\Delta C/T$ data.

material and in order to minimize the effect of eddy currents induced by the large $\mathrm{d}B/\mathrm{d}t$ rate in metals with very low resistivity, the material has been measured as a powder, fixed in electrical insulating paraffin. The powder samples have been oriented along the magnetic easy direction in a steady field of 4.8 T, applied above the paraffin's melting temperature. The orientation was checked by comparing the temperature dependence of the susceptibility of the powdered samples with that of single crystals measured along the easy direction.

3. Zero-field results

First, we concentrate on the high-temperature properties of $YbRh_2Si_2$. The magnetic susceptibility, measured along and perpendicular to the c-axis, follows a Curie–Weiss law above 200 K with an effective moment close to the value of free Yb^{3+} ($\mu_{\mathrm{eff}} = 4.5\mu_{\mathrm{B}}$) [17]. Due to strong magnetocrystalline anisotropy, there is a marked difference in the respective extrapolated values for the Weiss temperature indicating that the c-axis is the magnetic hard direction [17]. For Yb^{3+} ions in a tetragonal environment, a crystalline electric field (CEF) splitting of the $J = 7/2$ multiplet into four doublets is expected. Inelastic neutron-scattering experiments on $YbRh_2Si_2$ powder have found CEF excitations of the Yb^{3+} ions at approximately 17, 25 and 43 meV [18]. Thus, the doublet ground state is well separated from the first excited CEF level being located at around 200 K. This scheme is consistent with the magnetic specific-heat contribution, $\Delta C(T)$, derived by subtracting the specific heat of $LuRh_2Si_2$ from that of $YbRh_2Si_2$. Figure1 shows the specific-heat increment $\Delta C(T)/T$ on a logarithmic temperature scale and the integrated electronic or magnetic entropy $S_{\mathrm{m}}(T)$ of the Yb^{3+} ions is displayed in the inset. The full entropy expected for the $J = 7/2$ Yb^{3+} multiplet is recovered above room temperature. The single-ion Kondo temperature of the CEF doublet ground state can be roughly estimated from $S_{\mathrm{m}}(\frac{1}{2}T_{\mathrm{K}}) = \frac{1}{2}R\ln 2$, yielding $T_{\mathrm{K}} = 25$ K. Below about 10 K, the electronic specific-heat

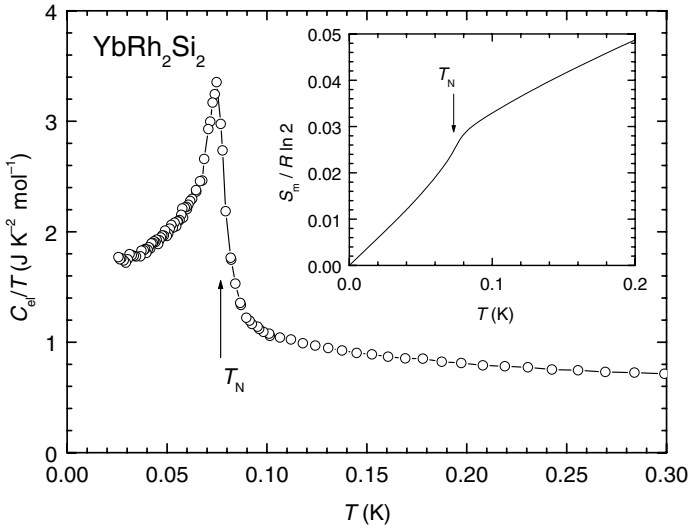

Figure 2. Low-temperature electronic specific heat of $YbRh_2Si_2$ as C_{el}/T versus T. C_{el} is obtained by subtracting a tiny nuclear quadrupolar contribution [5]. The inset displays the magnetic entropy in units of $R \ln 2$. Arrows indicate AF phase transition.

coefficient follows a logarithmic increase $\Delta C(T)/T \propto \ln(T_0/T)$ [3]. This non-Fermi liquid behaviour is related to the AF QCP in this system. T_0 may be interpreted as a characteristic spin-fluctuation temperature. As shown in figure 1, T_0 equals the single-ion Kondo temperature, as observed for many other HF systems close to AF QCPs [19].

At $T \approx 0.3$ K, the electronic specific-heat coefficient deviates from the logarithmic behaviour and follows a power-law divergence upon cooling towards the AF phase transition. As shown in figure 2, a clear mean-field-type anomaly is observed at T_N. Extrapolating $C(T)/T$ as $T \to 0$ to $\gamma_0 = 1.7$ J K^{-2} mol^{-1} reveals an entropy gain at T_N of less than $0.03R \ln 2$ (cf inset of figure 2), evidencing the weakness of the AF order in $YbRh_2Si_2$.

These results of the specific heat and entropy indicate that, for this system, there are at least two relevant and well-separated low-energy scales: the Kondo interaction ($T_K = 25$ K) and the very weak AF order ($T_N = 70$ mK). In the following, we will discuss the magnetic field effect on these two energy scales and use the results of low-temperature thermodynamic, magnetic and electrical-transport experiments to determine the magnetic field versus temperature phase diagram.

4. High-field behaviour

Figure 3 shows the low-temperature magnetization at several different hydrostatic pressures. $M(B)$ is strongly nonlinear both at very small fields close to the critical field B_c (cf inset of figure 3), as well as at large fields where the polarization amounts to approximately 1 μ_B per Yb-atom. Upon increasing the temperature to values above T_N, the low-field anomaly broadens and shifts to higher field values [14]. This results in broad maxima in the temperature dependence of the ac-susceptibility registered at constant fields [11, 14]. The considerable decrease in slope

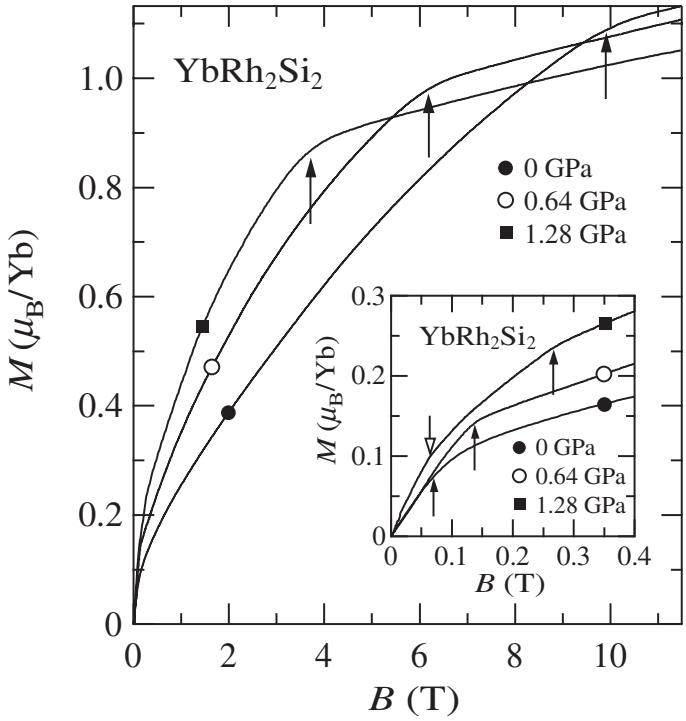

Figure 3. Isothermal magnetization ($B \perp c$) of $YbRh_2Si_2$ at differing pressures of 0, 0.64 and 1.28 GPa measured at 40, 40 and 60 mK, respectively [15]. Arrows indicate respective values of characteristic field B^*, see text. The inset enlarges the low-field regime. Arrows indicate critical fields for AF order.

of the magnetization curve occurs when the field has led to a partial (0.1 μ_B/Yb) polarization of fluctuating moments.

A second change of the magnetization curve is found around 10 T at ambient pressure. This upper 'kink' in $M(B)$ broadens rapidly with increasing temperature and disappears above 2 K without shifting its position in field [15]. As shown in figure 3, this anomaly is very sensitive to hydrostatic pressure: B^* shifts to 6.2 and 3.7 T at 0.64 and 1.28 GPa, respectively.

We now compare the pressure dependence of B^* with that of the characteristic spin fluctuation temperature T_0 estimated by fitting the specific-heat increment with $\Delta C(T)/T \propto \ln(T_0/T)$. Figure 4 displays $T_0(P)$ as determined from specific-heat measurements under hydrostatic pressure [20]. Since at ambient pressure T_0 matches with the single-ion Kondo temperature T_K determined from the magnetic entropy (cf figure 1), it is straightforward to assume that the pressure dependence of T_0 represents that of the Kondo temperature T_K in accordance with the exponential decrease of T_K with pressure. Thus, figure 4 indicates a close relation between T_K and the characteristic field B^* and suggests the Zeeman energy $g\mu_B B^*$ to equal the Kondo energy $k_B T_K$. This yields $g = 3.7 \pm 0.4$ in good agreement with the Yb-ESR derived g-factor observed below 20 K [13].

Using the isothermal compressibility $\kappa_T = 5.3 \times 10^{-12}$ Pa^{-1} [21], we obtain the 'thermal' Grüneisen parameter $\Gamma_T = 1/\kappa_T \times \partial \ln T_K/\partial P = -132 \pm 6$. The 'magnetic' Grüneisen parameter, derived from the pressure dependence of the characteristic field B^*, $\Gamma_B = 1/\kappa_T \times \partial \ln B^*/\partial P$, equals Γ_T because of the same slope for T_0 and B^* in their pressure dependences.

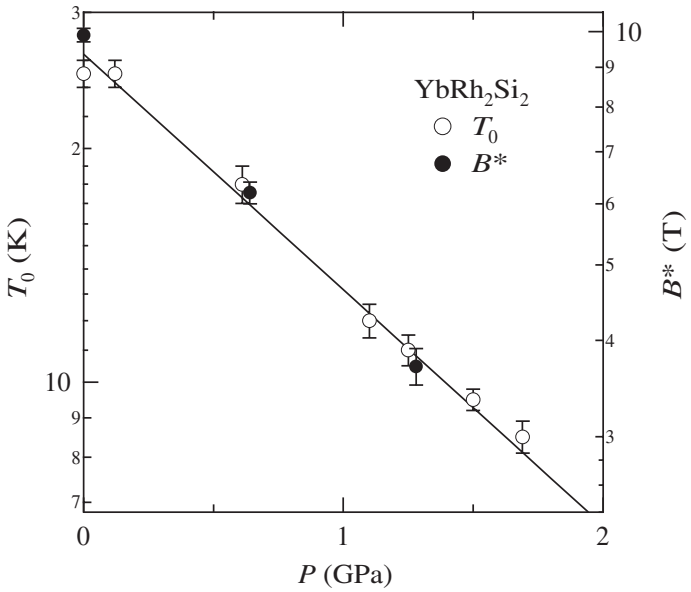

Figure 4. Comparison of the pressure dependence of the characteristic spin fluctuation temperature T_0 [20] (left axis) with that of the characteristic field B^* [15] (right axis) for $YbRh_2Si_2$ in a semi-logarithmic representation. The solid line represents $\exp(-0.7\ \mathrm{GPa}^{-1} \times P)$ dependence.

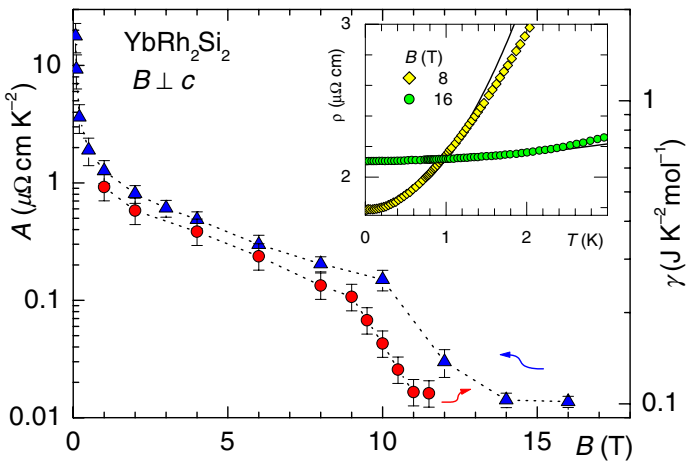

Figure 5. Field dependence of coefficients A (blue triangles, left axis) and γ (red circles, right axis; [15]) from LFL behaviour in the electrical resistivity ($\rho(T) = \rho_0 + AT^2$) and specific heat ($C(T)/T = \gamma$), respectively ($B \perp c$). The inset shows ρ versus T for 8 and 16 T. Solid lines represent T^2 behaviour [23].

This resembles the case of $CeRu_2Si_2$ for which Γ_B, determined from the pressure dependence of the metamagnetic transition, equals Γ_T as well [22].

To get more information on the properties of the heavy quasi-particles around B^*, we analyse the field dependence of the electronic specific-heat coefficient γ [15] and the coefficient A of the T^2 dependence of the electrical resistivity in the LFL regime. As shown in figure 5, a drastic

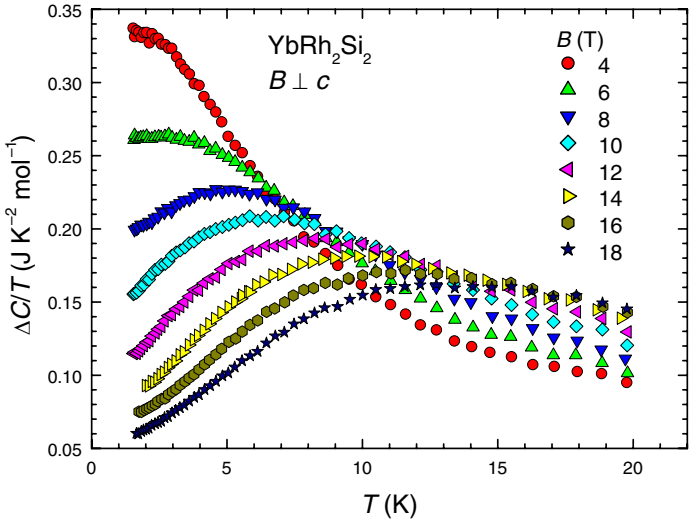

Figure 6. $4f$ increment to the specific heat of $YbRh_2Si_2$ as $\Delta C/T$ versus T for various magnetic fields applied perpendicular to the c-axis.

reduction of both properties is observed upon increasing the field from below to above B^*. The smallness of γ and A for $B > B^*$ indicates that the HF behaviour is suppressed beyond this field.

We have also investigated the field dependence of the specific heat at elevated temperatures. Figure 6 displays the specific-heat increment after subtraction of the phonon contribution, determined from the specific heat of $LuRh_2Si_2$ at fields between 4 and 18 T. At 4 T, the specific-heat coefficient $\Delta C(T)/T$ exhibits a maximum around 2 K which marks the cross-over from the non-Fermi liquid (NFL) to LFL behaviour observed previously [3, 5]. With increasing field, this maximum broadens and shifts to higher temperatures, indicating the shift of magnetic entropy. Such behaviour is known for Kondo systems under magnetic fields and can reasonably well be reproduced within the (single-ion) resonance-level model [24].

The suppression of HF behaviour for fields beyond B^* suggests that the effective Yb-valency reaches 3+ at high fields, also consistent with the large polarized moment observed in the dc-magnetization. In Yb-systems, the ionic radius of the magnetic Yb^{3+} configuration is smaller than that of the non-magnetic Yb^{2+} one. With increasing magnetic polarization, a decrease of the crystal volume is thus expected, as observed e.g. in the $YbCu_{5-x}Ag_x$ series [25]. We have studied the uniaxial length change $\Delta L(B)/L$ perpendicular to the c-axis at low temperatures. As shown in figure 7, a clear change in the slope of the length change is observed at B^*, corresponding to a step-like change of the magnetostriction coefficient $\lambda(B) = \mathrm{d}(\Delta L(B)/L)/\mathrm{d}B$. The overall negative length change is consistent with a smooth increase of the Yb-valency with increasing magnetic polarization. For $B < B^*$, the absolute value of the magnetostriction coefficient increases with increasing field. Then, at $B = B^*$, $|\lambda(B)|$ abruptly decreases and becomes field-independent. A qualitatively similar though more broadened anomaly has been found previously [23]. It suggests that the valency reaches 3+ beyond B^*, consistent with polarized f-electrons at high fields.

The decrease of T_K and B^* with hydrostatic pressure has been discussed above. A *negative* pressure effect, i.e. a volume expansion, can be obtained by replacing Rh by Ir: $YbIr_2Si_2$ [26]. Depending on synthesis conditions, this compound crystallizes either in the I-type body-centred

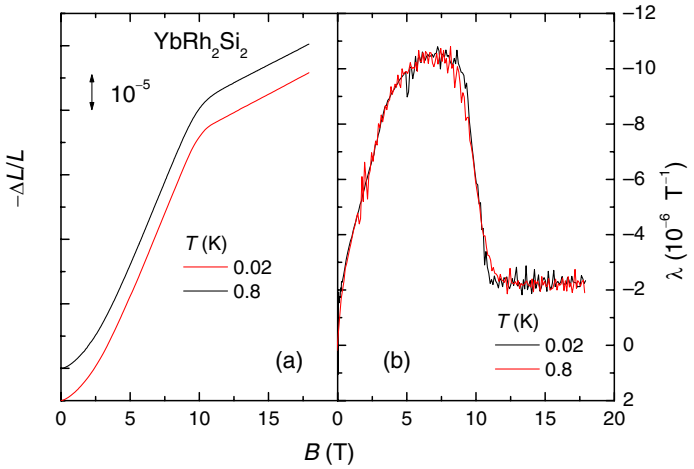

Figure 7. (a) Isothermal length change perpendicular to the c-axis for $YbRh_2Si_2$ as $\Delta L/L$ versus B ($B \perp c$) at 0.02 K (red line) and 0.8 K (black line). (b) Linear magnetostriction coefficient λ versus B for the same temperatures as in (a).

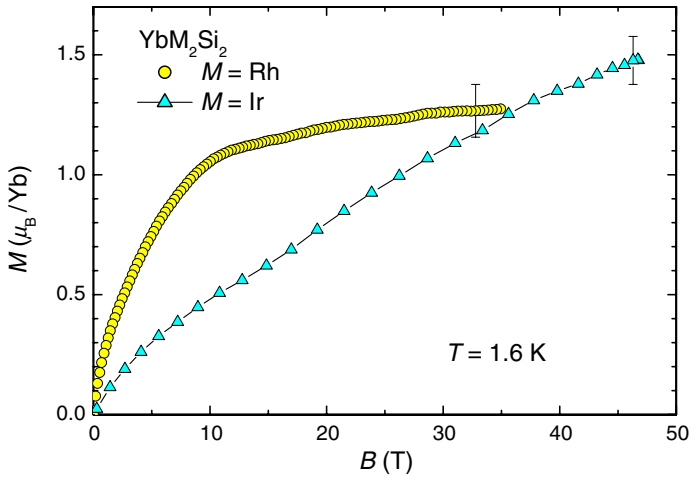

Figure 8. Magnetization M of $YbRh_2Si_2$ (yellow circles) and $YbIr_2Si_2$ (blue triangles) measured in pulsed fields at 1.6 K on oriented powder samples ($B \perp c$).

$ThCr_2Si_2$ or P-type $CaBe_2Ge_2$ structure. Whereas the P-type system has a low Kondo scale ($T_K = 2$ K) and orders magnetically at 0.7 K, the I-type system corresponds to slightly volume expanded $YbRh_2Si_2$ with a Kondo temperature of roughly 40 K [26]. Except for temperatures below about 0.3 K, where a cross-over to a paramagnetic LFL ground state takes place [26], the behaviour of $YbIr_2Si_2$ is qualitatively similar to that found for its Rh-homologue. It is thus interesting to investigate whether a high-field anomaly, corresponding to the suppression of HF behaviour under magnetic field, occurs in the Ir-system as well. Figure 8 shows pulsed-field magnetization data, taken at 1.6 K on both the Rh- and Ir-system. Whereas for the former, a clear change in slope occurs at 10 T, no corresponding anomaly can be resolved in the latter case, and the magnetization curve is much less steep. Since hydrostatic pressure results on $YbRh_2Si_2$ indicate that the magnetization signature at B^* weakens as B^* increases (cf figure 3),

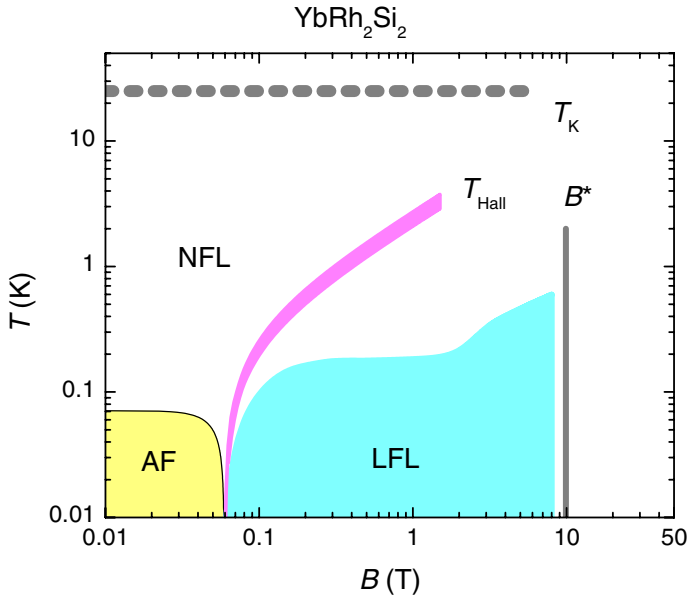

Figure 9. Double-logarithmic representation of the temperature versus magnetic field phase diagram for $YbRh_2Si_2$ ($B \perp c$). Dashed and solid grey lines display T_K (at $B = 0$) and B^*, derived from the zero-field specific heat and low-temperature magnetization [15], respectively. The sharp black line indicates boundary of AF phase [4]. The broad red line displays position of cross-over in the isothermal Hall resistance [8], which agrees with that of signatures in the isothermal magnetization and ac-susceptibility [11, 14] and marks the low-temperature boundary of the NFL region. The regime where the electrical resistivity follows LFL behaviour $\Delta\rho \propto T^2$ is marked in blue [4].

a corresponding anomaly for the Ir-system may not be detectable. In view of the twice larger T_K in the Ir-system, it is surprising that a polarization of 1 μ_B requires roughly four times larger fields. This may indicate substantially weaker FM fluctuations in the Ir compared to the Rh system.

In figure 9, we present the temperature versus field phase diagram for $YbRh_2Si_2$ as deduced from the various experiments discussed before. Corresponding to the two well-separated temperature scales observed at zero field, $T_K \approx 25$ K and $T_N = 70$ mK, two characteristic fields of $B_c = 0.06$ T and $B^* \simeq 10$ T have been found. Whereas the boundary of the AF state is determined by a line of second-order phase transitions, T_K and B^* mark the cross-over from local moment to HF behaviour. The field-induced suppression of the Kondo effect manifests itself in a kink in the magnetization and correspondingly steplike decrease of the susceptibility $\chi_0(B)$, electronic specific-heat coefficient $\gamma(B)$ and quasi-particle scattering cross-section $\sim A(B)$. Figure 9 also displays the cross-over line observed in the Hall resistivity. Upon decreasing the temperature, this feature sharpens, suggesting a sudden change of the Fermi surface volume at the field-induced QCP [8]. Upon increasing the field at constant temperature, the magnetization curve shows a considerable decrease in slope when passing this line, which indicates a partial (10%) FM polarization of fluctuating moments [14]. Correspondingly, broad maxima in the ac-susceptibility $\chi(T)$ are observed at characteristic temperatures which increase with increasing

field [11]. As discussed above, the spectrum of the quantum critical fluctuations in $YbRh_2Si_2$ is complicated and consists of both AF and FM components. The former dominate in the closest vicinity to the QCP ($T \leqslant 0.3$ K and $B \leqslant 0.15$ T) [11, 12], while the latter are observed in a broad range of the T–B phase diagram for temperatures below 10 K and magnetic fields below 10 T. The competition between AF and FM fluctuations may also be responsible for the absence of superconductivity close to the QCP even in the cleanest high-quality single crystals with a residual resistivity ratio exceeding 200.

5. Conclusion

We have studied the phase diagram of $YbRh_2Si_2$ by low-temperature magnetic, transport and thermodynamic measurements up to very high magnetic fields. In general, when the Zeeman energy $g\mu_B B^*$ becomes comparable to $k_B T_K$, the Kondo effect is suppressed and HF behaviour is destroyed. For $YbRh_2Si_2$, this leads to distinct anomalies which have not been observed in other HF metals yet: the magnetization shows a sharp change in slope, but this is not accompanied by any signature of metamagnetism. For HF systems with Ising-like spin anisotropy, e.g. $CeRu_2Si_2$ [2] or $CeCu_6$ [27], AF correlations dominate in the HF regime and their abrupt decrease at the field-induced suppression of the Kondo effect gives rise to metamagnetism for fields along the easy direction. For $YbRh_2Si_2$, by contrast, AF correlations are already suppressed at very small fields exceeding 0.15 T, and FM fluctuations dominate. Their polarization with increasing field causes a large magnetization already well below the transition at B^* and prevents any signature of metamagnetism. Probably, this behaviour which is strikingly different from that of the above-mentioned systems is related to the easy-plane spin anisotropy in $YbRh_2Si_2$. The latter may give rise to a (long wavelength) spiral structure along the c-axis in the AF ordered state and low-lying $q = 0$ fluctuations in the paramagnetic regime. Detailed neutron-scattering experiments are highly desirable and a possible relation between the strong FM fluctuations and the occurrence of a large Yb-ESR well below T_K in this system urgently needs to be clarified.

Acknowledgments

We are grateful to C Klausnitzer, T Nakanishi, M Nicklas and G Sparn for their support and advice for the use of the hydrostatic pressure cell. Stimulating discussions with E Abrahams, P Coleman, Z Hossain, K Ishida, K Neumaier, M Nicklas, S Paschen, C Pépin, T Radu, Q Si, J Sichelschmidt, O Stockert, T Tayama, K Tenya, O Trovarelli, H Wilhelm and S Wirth are gratefully acknowledged. Work at the Max Planck Institute for Chemical Physics of Solids supported in part by the Fonds der Chemischen Industrie and the COST Action P16 (ECOM). PK was supported by Bundesministerium für Bildung und Forschung project 03 SC 5 DRE.

References

[1] Doniach S 1977 *Physica* B **91** 231
[2] Flouquet J, Kambe S, Regnault L P, Haen P, Brison J P, Lapierre F and Lejay P 1995 *Physica* B **215** 77
[3] Trovarelli O, Geibel C, Mederle S, Langhammer C, Grosche F M, Gegenwart P, Lang M, Sparn G and Steglich F 2000 *Phys. Rev. Lett.* **85** 626

[4] Gegenwart P, Custers J, Geibel C, Neumaier K, Tayama T, Tenya K, Trovarelli O and Steglich F 2002 *Phys. Rev. Lett.* **89** 056402
[5] Custers J, Gegenwart P, Wilhelm H, Neumaier K, Tokiwa Y, Trovarelli O, Geibel C, Steglich F, Pépin C and Coleman P 2003 *Nature* **424** 524
[6] Küchler R *et al* 2003 *Phys. Rev. Lett.* **91** 066405
[7] Pépin C 2005 *Phys. Rev. Lett.* **94** 066402
[8] Paschen S, Lühmann T, Wirth S, Gegenwart P, Trovarelli O, Geibel C, Steglich F, Coleman P and Si Q 2004 *Nature* **432** 881
[9] Coleman P, Pépin C, Si Q and Ramazashvili R 2001 *J. Phys.: Condens. Matter* **13** R723
[10] Si Q, Rabello S, Ingersent K and Smith J L 2001 *Nature* **413** 804
[11] Gegenwart P, Custers J, Tokiwa Y, Geibel C and Steglich F 2005 *Phys. Rev. Lett.* **94** 076402
[12] Ishida K, Okamoto K, Kawasaki Y, Kitaoka Y, Trovarelli O, Geibel C and Steglich F 2002 *Phys. Rev. Lett.* **89** 107202
[13] Sichelschmidt J, Ivanshin V A, Ferstl J, Geibel C and Steglich F 2003 *Phys. Rev. Lett.* **91** 156401
[14] Gegenwart P, Tokiwa Y, Custers J, Geibel C and Steglich F 2006 *Proc. ASR-WYP-2005 Tokai* (*J. Phys. Soc. Japan* (Suppl.) in press)
[15] Tokiwa Y, Gegenwart P, Radu T, Ferstl J, Sparn G, Geibel C and Steglich F 2005 *Phys. Rev. Lett.* **94** 226402
[16] Krug H *et al* 2001 *Physica* B **294–295** 605
[17] Trovarelli O, Geibel C and Steglich F 2000 *Physica* B **284–288** 1507
[18] Stockert O, Koza M M, Ferstl J, Murani A P, Geibel C and Steglich F 2006 *Physica* B in press
[19] Sereni J, Geibel C, Berisso M G, Hellmann P, Trovarelli O and Steglich F 1997 *Physica* B **230–232** 580
[20] Mederle S, Borth R, Geibel C, Grosche F M, Sparn G, Trovarelli O and Steglich F 2002 *J. Phys.: Condens. Matter* **14** 1073
[21] Plessel J, Abd-Elmeguid M M, Sanchez J P, Knebel G, Geibel C, Trovarelli O and Steglich F 2003 *Phys. Rev.* B **67** 180303
[22] Lacerda A, de Visser A, Haen P, Lejay P and Flouquet J 1989 *Phys. Rev.* B **40** 8759
[23] Tokiwa Y, Gegenwart P, Weickert F, Küchler R, Custers J, Ferstl J, Geibel C and Steglich F 2004 *J. Magn. Magn. Mater.* (Suppl. 1) **272–276** e87
[24] Schotte K D and Schotte U 1975 *Phys. Lett.* A **55** 38
[25] Tsujii N, Mitamura H, Goto T, Yoshimura K, Kosuge K, Terashima T, Takamasu T, Kitazawa H, Kato S and Kido G 2001 *Physica* B **294–295** 284
[26] Hossain Z, Geibel C, Weickert F, Radu T, Tokiwa Y, Jeevan H, Gegenwart P and Steglich F 2005 *Phys. Rev.* B **72** 094411
[27] Löhneysen H v, Schlager H G and Schröder A 1993 *Physica* B **186–188** 590